IOPscience iopscience.iop.org

Home Search Collections Journals About Contact us My IOPscience

Preparation and photoluminescence of thin films of Ge nanoparticles embedded in Al_2O_3 matrices

This article has been downloaded from IOPscience. Please scroll down to see the full text article.

2001 J. Phys.: Condens. Matter 13 4075

(http://iopscience.iop.org/0953-8984/13/18/315)

View the table of contents for this issue, or go to the journal homepage for more

Download details:
IP Address: 171.66.16.226
The article was downloaded on 16/05/2010 at 11:56

Please note that terms and conditions apply.

INSTITUTE OF PHYSICS PUBLISHING JOURNAL OF PHYSICS: CONDENSED MATTER

J. Phys.: Condens. Matter **13** (2001) 4075–4080 www.iop.org/Journals/cm PII: S0953-8984(01)21607-5

Preparation and photoluminescence of thin films of Ge nanoparticles embedded in Al_2O_3 matrices

Y Zhu and P P Ong[1]

Department of Physics, National University of Singapore, 10 Kent Ridge Crescent, Singapore 119260

E-mail: phyongpp@nus.edu.sg

Received 7 February 2001, in final form 23 February 2001

Abstract

Thin films of Ge/Al_2O_3 were prepared using the pulsed laser deposition method. XRD and AFM confirmed that the structure consists of Ge nanoparticles embedded in amorphous Al_2O_3 matrices. A blue PL from the films was found in the wavelength region of 400–550 nm with two distinct humps in the peak. The origin of the PL is attributed to localized Ge/O-related interfacial defects. Our results show evidence that the amorphous Al_2O_3 matrices encapsulating the Ge nanocrystals provided them with a compact and air-tight seal preventing atmospheric oxygen from diffusing into the surface of the Ge nanoparticles even when the film was annealed at a high temperature.

1. Introduction

Group IV nanocrystals embedded in a SiO_2 matrix have been studied extensively because of their potential applications in integrated optoelectronic devices. Research on Ge nanocrystals embedded in a SiO_2 matrix is relevant for their application in novel optical devices [1–3]. Luminescent Ge nanocrystals (nc-Ge) have been fabricated by several groups using rf cosputtering, dc sputtering and ion implantation. The usual photoluminescence (PL) spectrum is a broad band centred at about 2.1–2.4 eV [2, 4].

Although SiO_2 is widely used in SiO_2-based gate dielectrics in logic and memory semiconductor electronic devices, and in single electronic and opto-electronic devices [5, 6], the aggressive shrinking of the thickness for gate dielectrics to below 2–3 nm brings about a number of fundamental problems involved in further oxide down-scaling, with the most critical ones being reduced dielectric reliability and exponentially increasing leakage current with decreasing oxide thickness [7]. In order to preserve quantum confinement within a silicon nanocrystal, the maximum concentration of nanoparticles in SiO_2 without encountering breakdown of electrical insulation between the nanoparticles is limited by the requirement that the spacing between adjacent nanoparticles should be no less than 2–3 nm. This has led to a search for alternative materials whose dielectric constant is higher than that of SiO_2 but whose other properties remain similar to SiO_2. Al_2O_3 is a good candidate for this application, as its band gap is similar to that of SiO_2 but its dielectric constant is more than twice as high.

[1] Corresponding author.

 © 2001 IOP Publishing Ltd Printed in the UK

Recently, the use of the pulsed laser deposition (PLD) method has been extended from the growth of epitaxial thin films to films containing granular particles. Silicon nanocrystalline thin films have been synthesized by laser ablation of silicon in 0.2–10 Torr background gases [8–11]. In this method, the background gases played an important role in the formation of the nanocrystalline particles. More recently, Geohegan *et al* [12] have reported the formation of nanoparticles during the expansion of the ablated plume following laser ablation.

In this paper, we report the Ge/Al_2O_3 thin films prepared by using a variation of the pulsed laser deposition method. No background gases surrounding the substrate were needed and the Ge and Al_2O_3 were evaporated alternately. XRD (x-ray diffractometry) and AFM (atomic force microscopy) results show that the as-prepared sample consists of Ge nanoparticles embedded in amorphous Al_2O_3 matrices. A blue PL was found in the wavelength region of 400–550 nm with two distinct humps in the peak. The origin of the PL from the films is attributed to the Ge/O-related defects. Furthermore, XPS results indicate that amorphous Al_2O_3 is a good host matrix for the prevention of oxidation of the Ge nanoparticles even when the film is annealed in the open atmosphere.

2. Experimental details

Details of the target and sample preparation are similar to those for the fabrication of thin films of Si nanoparticles embedded in Al_2O_3 matrices which was described in [13]. Briefly, a Nd:YAG pulsed laser was used to ablate the target in an ultrahigh vacuum chamber. The target to be laser ablated was first prepared from one piece of high purity (99.999%) small round Ge wafer and one 99.99% Al_2O_3 (diameter $D_2 = 25$ mm) round plate. The Ge wafer was glued onto the surface of the Al_2O_3 plate, making a two-layer assembly with only physical, not chemical, contact. During the PLD process, the centre of the Ge–Al_2O_3 target assembly was set to spin slowly about its central axis and the laser beam vaporized the two component materials alternately. All the glass substrates were first cleaned in an acetone ultrasonic bath and dried up. The growth of the thin films was carried out in a high vacuum system with a background pressure of about 8×10^{-8} mbar. The laser deposition was carried out for 40 minutes, with the target rotating at about 0.8 rotations/minute. The structures of the thin films were investigated by XRD performed on a PC-APD1729-1710 diffractometer using the Cu Kα line ($\lambda = 1.5418$ Å) and atomic force microscopy (AFM) (DI 3000 SPM with IIIa controller).

A set of five different samples was prepared for the XPS and PL study. These are the as-prepared pristine sample and the pristine samples annealed at 300, 400, 500 °C for 1 h, and at 500 °C for 6 h in the open but clean atmosphere, respectively. These samples will be referred to as samples (a)–(e) respectively. The same samples were used for the XPS and PL measurements. In order to ensure uniformity, all the as-prepared samples were cut from the same original sample which was sub-divided into several small pieces.

XPS measurements were carried out on a VG ESCALAB MKII spectrometer. A Mg Kα source (1253.6 eV photons) was used with the analyser mode set at a constant analyser energy of 20 eV. The x-ray source was run at 150 W (15 kV and 10 mA). The PL measurements were carried out with a fluorescence spectrophotometer (Perkin Elmer, LS 50B) using an excitation light wavelength of 380 nm (with a 300 W Xe lamp as the excitation source) for all the samples.

3. Results and discussion

Figure 1 shows the XRD results of the as-prepared sample. It can be seen that line peaks corresponding to Ge(111), Ge(220) and Ge(311) appeared as a superposition on the amorphous

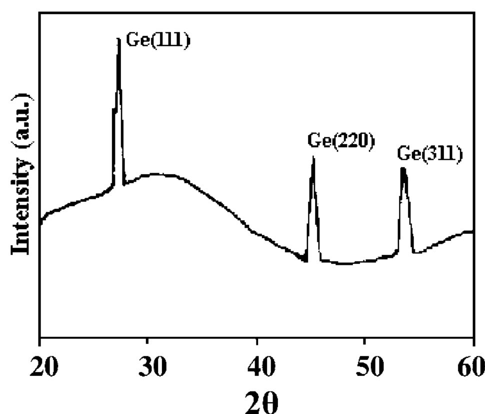

Figure 1. XRD results for the original sample.

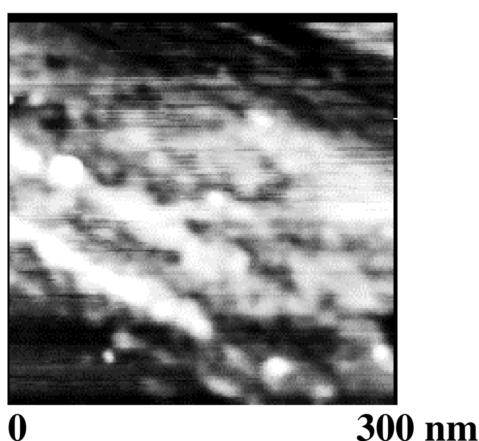

Figure 2. AFM image for the original sample.

background signal. The unresolved side peak in the Ge(111) peak suggests possible evidence of the presence of a GeO_2 peak which is mingled with the main Ge(111) peak. It is plausible to assume that the GeO_x crystalline structure exists at the interface between the Ge and its Al_2O_3 host. This assumption will be further confirmed by our XPS measurements below.

The average size of the nanoparticles was obtained from the Debye–Scherrer formula:

$$D = 0.9\lambda/B\cos\theta \tag{1}$$

where D is the average diameter of the nanocrystallites, λ is the wavelength of the x-ray source and B is the FWHM of the x-ray diffraction peak at the diffraction angle θ. We evaluated the mean diameter of the Ge nanocrystallites from the (220) peak to be about 25 nm for the sample. With XRD, it was difficult to deduce the size of the GeO_x crystalline structure as its peak was not resolved from the Ge(111) peak, and its intensity was too low for its width to be determined. However, AFM images of the $Ge(GeO_x)$ structure taken with a DI 3000 SPM with a IIIa controller and shown in figure 2 yield particle sizes of $Ge(GeO_x)$ roughly similar to those of the Ge crystals calculated from the XRD results. The XRD and AFM results are complementary since XRD cannot yield size information on the $Ge(GeO_x)$ crystalline structure while AFM cannot yield clear images of the Ge particles as they are embedded in the

amorphous Al_2O_3 matrices. Assuming that the GeO_x structures are formed at the boundaries of the Ge/Al_2O_3 interface, and combining the results of XRD for the Ge crystals and AFM for the $Ge(GeO_x)$ crystals, we can conclude that the as-prepared films are composed of tiny $Ge(GeO_x)$ crystals with diameters of about 25 nm embedded in amorphous Al_2O_3 matrices.

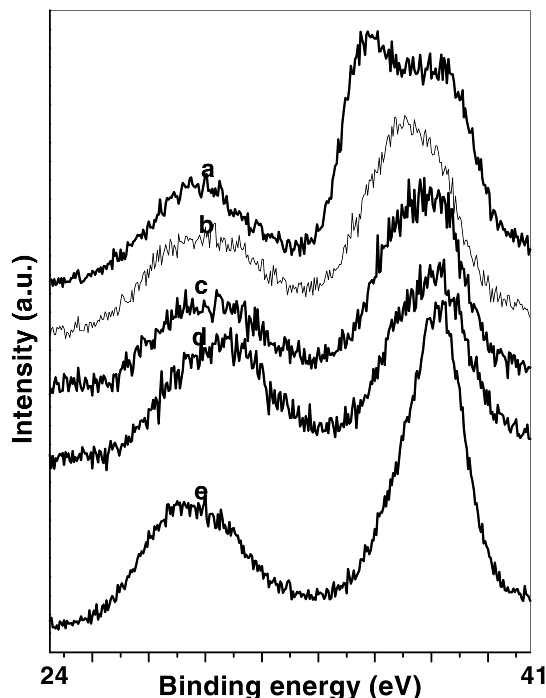

Figure 3. XPS results for the Ge 3d peaks for all the samples: (a) original as-prepared sample; (b) sample annealed at 300 °C for 1 h; (c) sample annealed at 400 °C; (d) sample annealed at 500 °C for 1 h and (e) sample annealed at 500 °C for 6 h. The samples were annealed in the open but clean atmosphere.

As all the samples consisted of only compositions of aluminum, Ge and oxygen (except for minor residual absorption compositions on the film surfaces), and since aluminum and oxygen do not produce much change in their XPS peaks, we therefore focused our attention on the changes in the Ge peaks. Figure 3 shows the XPS results for the Ge 3d peaks for all the five samples measured. Curve (a) represents the results for the as-prepared sample, while curves (b), (c), (d) and (e) are for the corresponding annealed samples. A small energy scale correction against charge effect was applied for the x-axis. In order to avoid overlapping of the curves, they are arbitrarily displaced vertically with respect to one another. All spectra were normalized to their peak values with respect to their base lines at about 24 eV. There are two broad peaks appearing in the Ge 3d spectra, the lower energy peak corresponding to Ge and the higher binding energy peak to GeO_x. The relative intensity of the lower energy part of the high energy peak decreased very much as the annealing temperature of the sample was increased, and it almost disappeared after the sample was annealed at 500 °C for 6 hours.

Our XPS measurements reveal a great difference between the respective GeO_x peaks (higher binding energy peaks) of the different samples that have been variously annealed, thus suggesting much change in the surface structures of the samples upon annealing. The peak becomes increasingly narrower and taller relative to that for the lower binding energy as the

annealing temperature was increased. Its position also shifted towards the high energy end with increasing annealing temperature. In comparison, there is hardly any change in position of the Ge peaks (low binding energy peaks) for the different samples. These results prove that when the sample annealing temperature was increased the GeO_x composition at the surface changed considerably, but the inner Ge layer of the film remained unoxidized. Indeed, even after the sample had been annealed in the atmosphere at 500 °C for 6 hours, there was still not much change in the pure Ge peak of the spectrum. This represents strong evidence that the amorphous Al_2O_3 matrices encapsulating the Ge nanocrystals provided them with a compact and air-tight seal preventing atmospheric oxygen from diffusing into the Ge surface even at a high temperature. There are two possible processes to account for the change of the GeO_x peak with various annealings. Firstly, the Ge nanoparticles which were located at the surface and not embedded inside the Al_2O_3 matrices would be gradually oxidized by the environmental oxygen. Secondly, there existed a net migration of oxygen from sites of low oxygen contents which donate their oxygen atoms to other sites acting as oxygen acceptors, thereby causing a displacement in the GeO_x peak. Both these processes contribute to a gradual shift in the GeO_x peak towards the high binding energy end with increasing intensity of annealing.

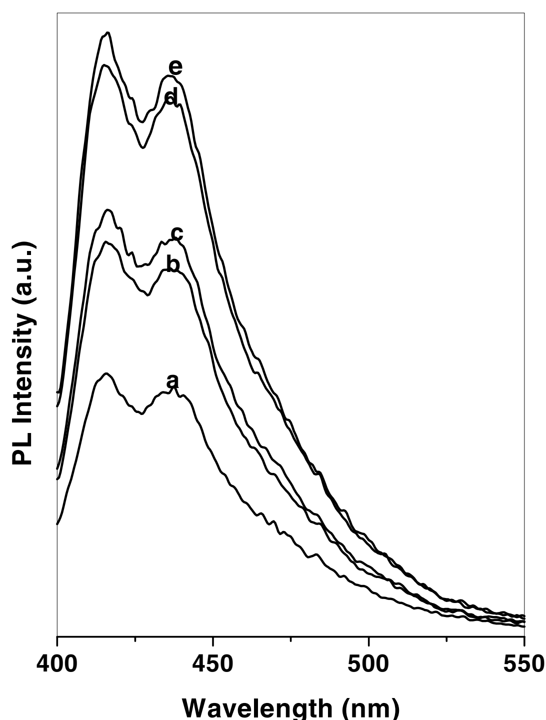

Figure 4. PL results for the samples (a)–(e) as defined in figure 3.

Figure 4 shows the PL results of all the samples in the wavelength region of 400–550 nm. It clearly shows two humps in the peak for the spectra of all the samples. In order to compare meaningfully, all measurements were made under the same conditions, and the same set of samples as in the XPS measurements were used. For the sample annealed at 300 °C for 1 hour (sample (b)), the PL intensity increased to about 1.5 times that of the unannealed sample. With sample (c) which was annealed at 400 °C for 1 hour, the PL intensity was only slightly raised further than that of sample (b). For sample (d), annealed at 500 °C for 1 hour, the PL intensity

increased to nearly 2.2 times that of the original unannealed one. For sample (e), annealed at 500 °C for 6 hours, the PL intensity was only slightly further raised from that of sample (d). In all cases, only the PL intensity changed, not the peak shape or position.

Comparing the PL and XPS results, it is possible to explain that the PL origin is related to the Ge/O interfacial structures. Although our thin films were prepared in vacuum, the Ge nanoparticles were initially partly oxidized, as confirmed by XPS. Some Ge/O structures already existed in the as-prepared film so that the PL peak appeared, but its intensity was low. After annealing of the sample, oxygen atoms inter-diffused from low oxygen sites to high oxygen sites in the GeO_x structures. The Ge nanoparticles in the Al_2O_3 matrices interact with the neighbouring oxygen particles. The higher the annealing temperature, the more oxygen inter-diffusion takes place, and the more opportunity for Ge nanoparticles to interact with neighbouring oxygen, leading to more Ge/O-related defects and a resulting increase in the PL intensity. These Ge/O-related defects in the GeO_x structures possibly contain two nonbonding electrons, which is similar to the Ge-doped silica glass fibres—as reported by Ginzburg *et al* [14] and Gallagher *et al* [15]. These two nonbonding electrons may have different excited states so that two humps in one peak appeared in the PL spectra of all the samples.

4. Conclusion

In conclusion, we have prepared Ge nanocrystals embedded in amorphous Al_2O_3 matrices. The origin of the blue PL is attributed to Ge/O related-defects in the film. With increasing intensity of annealing, the concentration of Ge/O defects increases leading to a corresponding increase in the intensity of blue PL. The amorphous Al_2O_3 matrix is a good host for the Ge nanocrystals providing them with a compact and air-tight seal which prevents atmospheric oxygen from diffusing into the Ge surface even at a high temperature.

Acknowledgments

We would like to thank Dr Q T Li for the use of the PL apparatus, and Ms B K Tan, Ms Y J Liu and Messrs H H Teo and H K Wong for their experimental assistance. This work was supported under NUS research grant no R-144-000-011-012.

References

[1] Fuji M, Hayashi S and Yamamoyo K 1991 *Japan. J. Appl. Phys.* **30** 687
[2] Paine D C, Caragianis C, Shigesato T and Ishikawa T 1993 *Appl. Phys. Lett.* **62** 2842
[3] Maeda Y, Tsukamoto N, Yazawa Y, Kanemitsu Y and Masumoto Y 1991 *Appl. Phys. Lett.* **59** 3168
[4] Maeda Y 1995 *Phys. Rev.* B **51** 1658
[5] Zhang L, Guo L and Chou S Y 1998 *Appl. Phys. Lett.* **72** 1205
[6] DiMaria D J, Kirtley J R, Pakulis E J, Dong D W, Kuan T S, Pesavento F L, Theis T N and Cutro J A 1984 *J. Appl. Phys.* **56** 401
[7] Muller D A, Sorsch T, Moccio S, Baumann F H, Evans-Lutterodt K and Timp G 1999 *Nature* **339** 758
[8] Chiu L A, Seraphin A A and Kolenbrander K D 1994 *J. Electron. Mater.* **23** 347
[9] Movtchan I A, Marine W, Dreyfus R W, Le H C, Sentis M and Autric M 1996 *Appl. Surf. Sci.* **96–98** 251
[10] Yamada Y, Orii T, Umezu I, Takeyama S and Yoshida T 1996 *Japan. J. Appl. Phys.* I **35** 1361
[11] Li S, Silvers S J and El-Shall M S 1997 *J. Phys. Chem.* B **101** 1794
[12] Geohegan D B, Puretzky A A, Duscher G and Pennycook S J 1998 *Appl. Phys. Lett.* **72** 2987
[13] Zhu Y, Wang H and Ong P P 2000 *J. Phys. D: Appl. Phys.* **33** 2687
[14] Ginzburg L P, Gordeev A A, Gorchakov A P and Jilinsky A P 1995 *J. Non-Cryst. Solids* **183** 234
[15] Gallagher M and Osterberg U 1993 *J. Appl. Phys.* **74** 2771